the plant journal

SEB Society for Experimental Biology

The Plant Journal (2016) **85,** 209–218 doi: 10.1111/tpj.13095

ABCB19-mediated polar auxin transport modulates Arabidopsis hypocotyl elongation and the endoreplication variant of the cell cycle

Guosheng Wu, Jacqueline S. Carville† and Edgar P. Spalding*

Department of Botany, University of Wisconsin-Madison, 430 Lincoln Drive, Madison, WI 53706, USA

Received 1 October 2015; revised 19 November 2015; accepted 24 November 2015; published online 10 December 2015.
*For correspondence (e-mail spalding@wisc.edu).
† Present address: ImmunoChemistry Technologies, LLC, 9401 James Avenue South, Suite 155, Bloomington, MN 55431, USA.

SUMMARY

Elongation of the Arabidopsis hypocotyl pushes the shoot-producing meristem out of the soil by rapid expansion of cells already present in the embryo. This elongation process is shown here to be impaired by as much as 35% in mutants lacking ABCB19, an ATP-binding cassette membrane protein required for polar auxin transport, during a limited time of fast growth in dim white light beginning 2.5 days after germination. The discovery of high ectopic expression of a cyclin B1;1-based reporter of mitosis throughout *abcb19* hypocotyls without an equivalent effect on mitosis prompted investigations of the endoreplication variant of the cell cycle. Flow cytometry performed on nuclei isolated from upper (growing) regions of 3-day-old hypocotyls showed ploidy levels to be lower in *abcb19* mutants compared with wild type. *CCS52A2* messenger RNA encoding a nuclear protein that promotes a shift from mitosis to endoreplication was lower in *abcb19* hypocotyls, and fluorescence microscopy showed the CCS52A2 protein to be lower in the nuclei of *abcb19* hypocotyls compared with wild type. Providing *abcb19* seedlings with nanomolar auxin rescued their low CCS52A2 levels, endocycle defects, aberrant cyclin B1;1 expression, and growth rate defect. The *abcb19*-like growth rate of *ccs52a2* mutants was not rescued by auxin, placing CCS52A2 after ABCB19-dependent polar auxin transport in a pathway responsible for a component of ploidy-related hypocotyl growth. A *ccs52A2* mutation did not affect the level or pattern of cyclin B1;1 expression, indicating that CCS52A2 does not mediate the effect of auxin on cyclin B1;1.

Keywords: ***Arabidopsis thaliana*, hypocotyl growth, ploidy, endocycle, CCS52A.**

INTRODUCTION

Plant growth and development continuously balances the fundamental processes of cell proliferation, expansion, and differentiation, each of which auxin and auxin transport helps coordinate (Santner and Estelle, 2009; Vanneste and Friml, 2009). The Arabidopsis seedling hypocotyl has proven useful for studying aspects of this coordination. Auxin in hypocotyls is mainly synthesized in the shoot apex and then transported rootward, or basipetally, where it can regulate cell expansion including differentially across the stem during tropisms (Spalding, 2013). Previous studies have shown a membrane protein of the ATP-binding cassette superfamily, ABCB19 (hereafter B19), to be necessary for 80% of the polar auxin stream in the Arabidopsis hypocotyl (Noh *et al.*, 2001). By impairing this auxin stream, *b19* mutations reduce the growth-controlling level of auxin in the hypocotyl, which renders photoreceptor-mediated inhibition of elongation more effective during de-etiolation (Wu *et al.*, 2010a). This genetic evidence supported previous pharmacology-based conclusions about polar auxin transport promoting growth in opposition to the inhibitory effects of the cryptochrome and phytochrome photosensory systems (Jensen *et al.*, 1997).

For decades, studies of auxin effects on stem elongation utilized excised segments of pea epicotyls, cucumber hypocotyls, and oat coleoptiles. Recently, auxin promotion of growth was also demonstrated in excised Arabidopsis hypocotyl segments (Takahashi *et al.*, 2012). Old and new results are consistent with the view that auxin leads to apoplast acidification, which promotes the activity of wall-loosening expansin proteins, which results in a rapid increase in growth rate (Rayle and Cleland, 1992; Cleland, 1995). Remarkably, a demonstration of exogenous auxin positively affecting elongation of an intact plant stem over longer time frames may not have been achieved until a

wick-based flow-through treatment was applied to pea plants (Yang *et al.*, 1993). The difference between the behavior of intact plants and stem segments was classically attributed to the need to deplete auxin levels by removing the segment from its auxin supply, principally the apical meristem, before a restorative effect of exogenous auxin could be detected. In these experimental scenarios, auxin promotes cell expansion up to an optimal concentration beyond which it is inhibitory.

Despite recent major advances in understanding auxin receptor-mediated signaling (Bargmann and Estelle, 2014) and the participation of small auxin up-regulated RNAs in auxin action (Chae *et al.*, 2012; Spartz *et al.*, 2012), it is still not clear how auxin controls hypocotyl growth. Unlike the growth of leaves or roots, which depends on the production of new cells by a tightly controlled cell cycle (De Veylder *et al.*, 2007; Gutierrez, 2009; Desvoyes *et al.*, 2014), hypocotyl cells rarely undergo mitosis except in the few epidermal cells that produce stomata (Gendreau *et al.*, 1997). Post-germination growth is essentially a manifestation of cell expansion. In the short term, the acid-growth mechanism is usually invoked to explain effects of auxin on cell expansion. Over longer time frames, polyploidy resulting from endoreplication of the nuclear genome has been linked to expansion of cells (Gutierrez, 2009). Polyploidy resulting from the endocycle variant of the cell cycle is found in most mature tissues in Arabidopsis (Galbraith *et al.*, 1991). It positively correlates with cell size (Melaragno *et al.*, 1993; Kondorosi *et al.*, 2000; Sugimoto-Shirasu and Roberts, 2003) and is influenced by environmental factors such as light (Gendreau *et al.*, 1998). The present study uses mutations in the B19 transporter to impair auxin flow down the Arabidopsis hypocotyl as a tool to investigate the coupling between auxin, hypocotyl elongation, and the endocycle.

RESULTS

Auxin transport regulates the nuclear endocycle in hypocotyl cells

The surprising observation that instigated the present study was very strong and ectopic expression of a mitosis marker gene, *proCYCB1;1:CYCB1;1-GUS* (Colón-Carmona *et al.*, 1999) in hypocotyls of *b19-1* mutants (Figure 1). This marker is used to visualize the pattern of endogenous CYCB1;1 which accumulates during the G2 to M phase of the cell cycle (Shaul *et al.*, 1996). Instead of the signal being restricted to the shoot apical meristem and scattered locations within the young cotyledons as is typical of the wild type (Figure 1a), *b19–1* hypocotyls displayed a strong signal throughout the seedling, particularly in the upper hypocotyl (Figure 1b). This signal is apparently distributed across the epidermis, cortex and central cylinder (Figure 1b inset). This reporter-gene phenotype was detectable

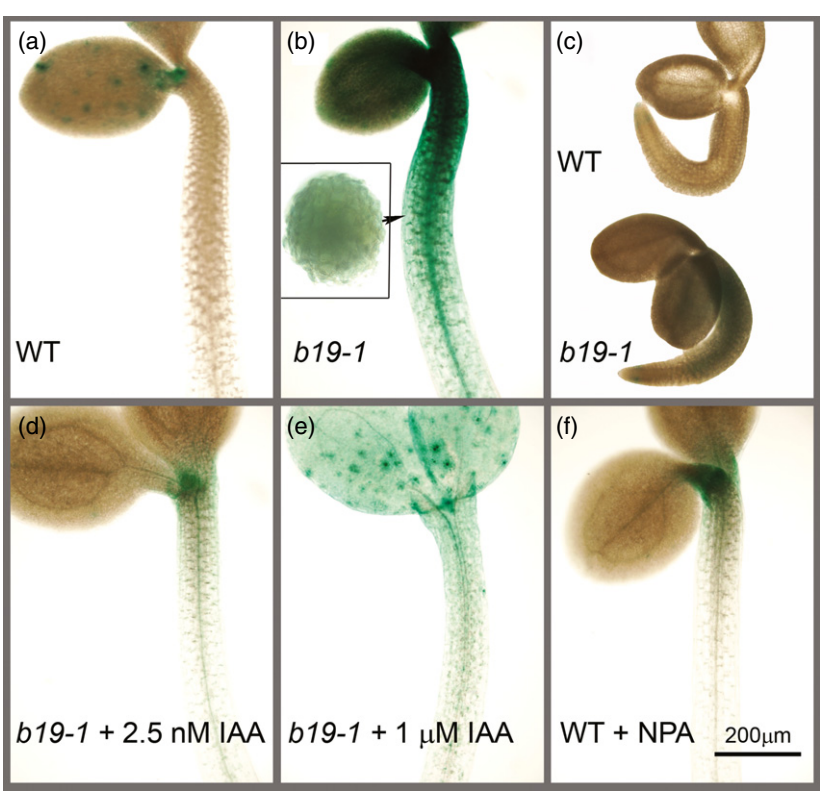

Figure 1. Auxin transport determines the expression pattern of a cycle reporter gene.
Compared with WT (a), CYCB1;1–GUS expression is strongly up-regulated in the hypocotyl of *b19-1* mutant seedlings (b) grown for 2.5 DAG in 10 μmol m^{-2} sec^{-1} white light. The inset shows a *b19-1* hypocotyl cross-section. This phenotype also is apparent in 1-day-old seedlings (c). Auxin application rescues the reporter-gene phenotype (d, e), and the auxin transport blocker NPA partially phenocopies the mutant (f).

as early as 1 day after germination (Figure 1c). If this cyclin promoter phenotype of *b19* was related to auxin deficiency caused by the well documented defect in polar auxin transport down the hypocotyl from a major site of synthesis at the shoot apex (Noh *et al.*, 2001; Geisler *et al.*, 2005; Spalding, 2013), auxin treatment would be expected to restore normal *CYCB1;1* reporter-gene signal patterns in the mutant. Auxin treatment indeed rescued the reporter-gene pattern, particularly faithfully when presented at the extremely low concentration of 2.5 nM or 1 μM IAA (Figure 1d,e). Moreover, treatment of the wild type with naphthylphthalamic acid (NPA), an inhibitor of polar auxin transport, caused an upregulation and abnormal spread of the reporter-gene signal, partially phenocopying the *b19* mutant (Figure 1f). At the mRNA level, the reporter gene was expressed similarly in the mutant and wild type (WT 1.00 ± 0.16 versus *b19* 1.32 ± 0.44, *P*-value = 0.54) as determined by quantitative PCR. The native *CYCB1;1* gene was not overexpressed in *b19* relative to wild type (Figure S1). These transcript analyses indicate that the conspicuous spread of the *proCYCB1;1:CYCB1;1-GUS* signal is due to defective degradation of the protein mediated by the destruction box domain of the *CYCB1;1* coding sequence (Colón-Carmona *et al.*, 1999). The endogenous CYCB1;1 protein is expected to share this reporter signal pattern.

Hypocotyls are not expected to display mitotic markers because cell divisions after embryogenesis are restricted to the few scattered epidermal cells forming stomata and rarely in the central cylinder (Gendreau *et al.*, 1997). Therefore, the auxin-dependent C*YCB1;1* reporter phenotype in an organ consisting almost entirely of non-dividing cells was considered an important phenomenon to understand. We began by determining if mitosis was occurring ectopically where the reporter was active. The number of cortical cells in a file the length of the hypocotyl was the same for wild type (33 ± 2; *n* = 20 seedlings) and *b19-1* (33 ± 1; *n* = 20 seedlings). The mean number of stomata along one flank of a *b19-3* hypocotyl (1.7 ± 0.5, *n* = 7) was lower (*P* < 0.05) than the wild-type value (3.5 ± 0.5, *n* = 8). Thus, high ectopic expression of a mitotic marker in *b19* was not associated with increased frequency of cell division. An alternative hypothesis, that *CYCB1;1* misregulation indicates an effect on the endocycle, a variant of the cell cycle in which doubling of the nuclear genome is not followed by cytokinesis (De Veylder *et al.*, 2011), was tested first by measuring nuclear size in cortical cells of the upper hypocotyl because ploidy and nuclear size may be correlated (Jovtchev *et al.*, 2006). Figure 2a shows representative *b19-1* nuclei marked by H2B–YFP in cortical cells of the upper hypocotyl. They appeared smaller than wild-type nuclei. The probability distribution functions fitted to manual measurements of wild-type and *b19* nuclear sizes from confocal microscopy images differed to a statistically-significant degree (*P* < 0.01) as determined by a Kolmogorov–

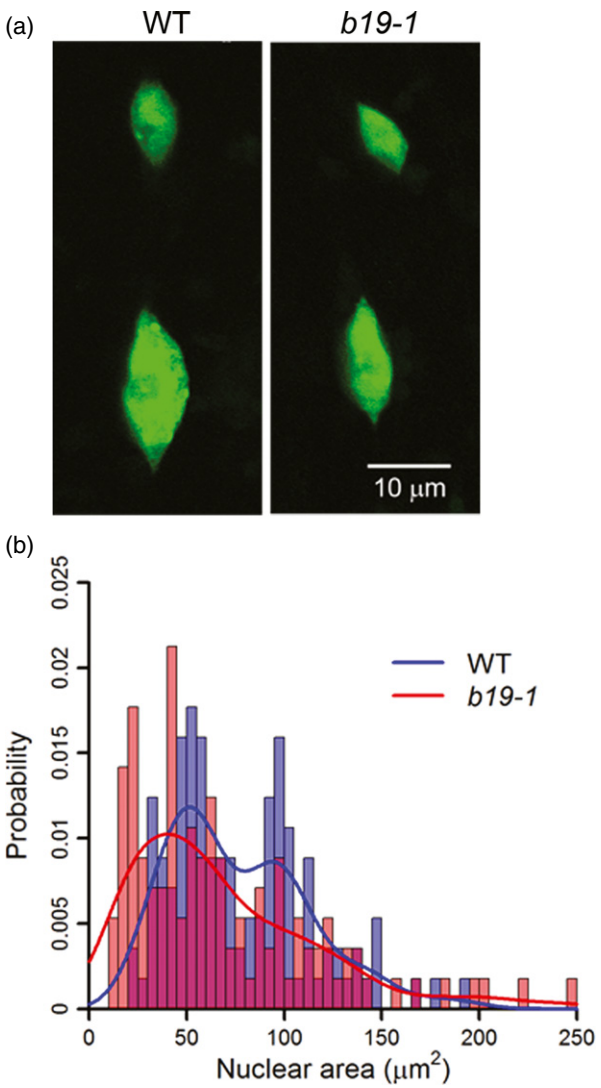

Figure 2. Smaller nuclei in cells of *b19* upper hypocotyls.
The *H2B–YFP* fluorescent nuclear marker was crossed into *b19-1* plants to visualize the nuclei.
(a) Representative confocal microcopy images of nuclei in the cortex of the upper hypocotyl of 2.5–3 DAG seedlings from which nuclear area was manually measured.
(b) Histograms of WT and *b19* nuclear areas show the wild-type distribution is shifted to larger sizes. Probability density functions (lines) derived were significantly different at *P* < 0.01. WT *n* = 114; *b19 n* = 156.

Smirnov test, and showed that nuclei from *b19* hypocotyls on average were smaller than wild type (Figure 2b). The *b19* distribution displayed less evidence of peaks corresponding to higher ploidy levels than wild type. Therefore, ploidy levels were more directly examined by measuring nuclear DNA content in populations of *b19* and wild-type nuclei by flow cytometry. Figure 3(a) shows a representative frequency histogram of the fluorescence signals from a population of upper-hypocotyl nuclei measured by flow cytometry. The peaks clearly distinguish the different

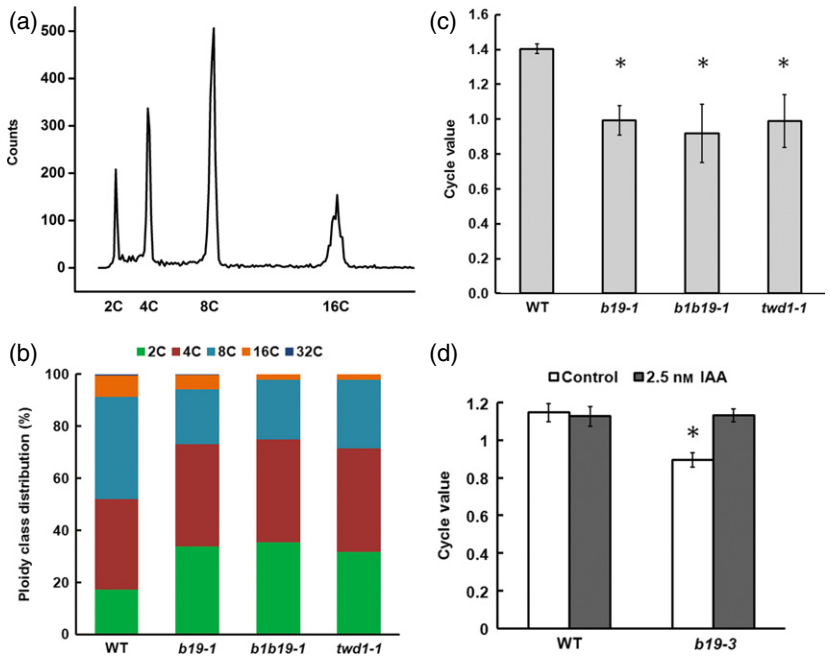

Figure 3. Reduced endoreplication in *b19* hypocotyls compared with wild type.
(a) Representative histogram of flow cytometry readings (DNA content) of a population of nuclei isolated from the upper hypocotyl shows clear separation of ploidy classes.
(b) Relative frequency of multiploid nuclei classes observed in different genotypes.
(c) Cycle values determined for each genotype from the data in (b).
(d) 2.5 nM auxin rescues the ploidy phenotype in *b19*.
Error bars indicate standard error of the mean ($n = 4$ biological replicates). Significant differences between WT and mutants are indicated with *(P-value < 0.05). The ecotype background is Ws for the genotypes represented in panels (b, c) and Col-0 in panel (d).

ploidy classes for individual nuclei. From the histograms it was determined that nuclei isolated from the upper region of *b19* hypocotyls are more likely to have two copies of the genome (2C) and less likely to have 8C than the wild type (Figure 3b). A double mutant in which the related *ABCB1* gene is also disrupted (*b1 b19*), which more severely inhibits polar auxin transport in hypocotyls (Noh *et al.*, 2001), displayed a slightly stronger ploidy phenotype as evidenced by the lack of the highest detectable 32C category of nuclei. The *TWD1* gene encodes an immunophilin protein that is required for proper trafficking of B1 and B19 to the plasma membrane (Bouchard *et al.*, 2006). Morphologically, *b1 b19* and *twd1* mutants are almost indistinguishable due to missing or mislocalized ABCB proteins, respectively (Wu *et al.*, 2010b). Figure 3(b) shows that the ploidy distributions in *twd1-1* nuclei are essentially indistinguishable from those isolated from *b1 b19* double mutants. A formula can convert the class distributions show in Figure 3(b) to the average number of nuclear doublings that have occurred in the populations of nuclei, a metric known as the cycle value or endoreplication index. Interpretation of this value assumes no mitosis, which was verified in the cortex where we expect most of the sampled nuclei originate. Figure 3(c) shows cycle values calculated from the results shown in Figure 3(b) to capture the low ploidy phenotype of the auxin-transport mutants in a single value. Figure 3(d) shows that treatment of intact hypocotyls with 2.5 nM IAA did not affect the cycle value of wild-type nuclei but completely rescued the *b19-3* nuclear defect. Because evidence of mitosis was not observed, these cycle value differences can be interpreted as differences in rates of endoreplication. Thus, impaired polar auxin transport through the hypocotyl results in misregulation of the *CYCB1;1* reporter gene and lower endocycle activity.

The molecular basis of the auxin transport effect on the endocycle

A survey of cell-cycle gene expression was conducted in wild-type and *b19* upper hypocotyls to learn more about the effects of altered auxin transport on the molecules controlling mitosis exit and endocycle entry (Lammens *et al.*, 2008). Quantitative PCR was used to measure the mRNA levels of 16 cyclin genes expected to be relevant in hypocotyls based on expression data (http://bar.utoronto.ca/efp/cgi-bin/efpWeb.cgi). Of the cyclin genes tested, *CYCD4;1* and *CYCD4;2* were significantly down-regulated in *b19* (Figure S1a). Similar results were obtained in a second allele of *b19* in a different ecotype background (Figure S1b). These gene expression phenotypes were rescued by 2.5 nM IAA (Figure S1b). In Arabidopsis, these two cyclins form active kinase complexes with CDKA;1 that promote G1/S and G2/M transitions (De Veylder *et al.*, 2011). The lower ploidy and the fewer stomata in *b19* may result from reduced CYCD4 levels, which appear to be the result of reduced auxin transport.

The onset of endoreplication requires the multisubunit E3 ubiquitin ligase known as the anaphase-promoting complex/cyclosome (APC/C) to degrade mitotic cyclins (Cebolla *et al.*, 1999; Zheng *et al.*, 2011). In Arabidopsis, three CELL CYCLE SWITCH 52 proteins known as CCS52A1, CCS52A2 and CCS52B form part of the APC/C and influence its activity and substrate specificity (Fülöp *et al.*, 2005; De Veylder *et al.*, 2011). The abnormally high activity of the *CYCB1;1* reporter and the lower ploidy in *b19* hypoco-

tyls (Figures 1–3) are possibly the result of low levels of the CCS52 activators and therefore low APC/C activity in the mutant. To investigate this potential explanation, we measured mRNA levels of *CCS52A1, CCS52A2* and *CCS52B* in upper-hypocotyl sections. Only *CCS52A2* expression was detected in the wild type. Its mRNA level was significantly lower in *b19* and wild-type seedlings treated with NPA (Figure 4a). Treatment with IAA (2.5 nM or 1 μM) rescued the *CCS52A2* expression phenotype of the *b19* mutant. The auxin-insensitive mutant *axr3–1* also displayed lower *CCS52A2* expression. The CCS52A2 protein level was also lower in *b19* and NPA-treated wild-type seedlings, as determined by measuring GFP fluorescence in nuclei of transgenic plants expressing a previously characterized functional CCS52A2–GFP fusion under the control of its native promoter (Vanstraelen *et al.*, 2009). As a control, the H2B–YFP fluorescent histone (Boisnard-Lorig *et al.*, 2001) was not affected by loss of B19 or NPA treatment (Figure 4b,c). Collectively, these results indicate that polar auxin transport controls CCS52A2 expression in a manner that may explain the *CYCB1;1* reporter phenotype observed in *b19.* A genetic test of this hypothesis was arranged by crossing the *proCYCB1;1:CYCB1;1–GUS* reporter into a *ccs52a2* mutant. Figure 5 shows the pattern of CYCB1;1 accumulation visualized by GUS staining was clearly not affected by the *ccs52a2* mutation. A phenocopy of the *b19* CYCB1;1 pattern was not observed. The result indicates that lowering CCS52A2 levels is not sufficient to cause ectopic overexpression of CYCB1;1. A linear pathway in which auxin delivered by ABCB19-dependent polar transport promotes the CCS52A2-dependent E3 ligase that degrades CYCB1;1 to restrict its expression pattern is not supported.

Hypocotyl elongation, auxin transport, and ploidy

The relationship between ABCB19-dependent auxin transport, hypocotyl elongation, and cycle value was tested here by acquiring digital time-lapse images and analysis utilizing the HYPOTrace software tool (Wang *et al.*, 2009), following the methods Wu *et al.* (2010a) used to study the connections between ABCB19-dependent auxin transport and the photocontrol of hypocotyl elongation. Figure 6(a) shows that wild-type and *b19* seedlings differed in growth rate most significantly between 2.5 and 3 days after germination, which was also the period of fastest hypocotyl elongation. These results were used to design image-based assays of growth rate specifically over the 2.5–3 days time period to determine the effects of auxin. A dose–response analysis demonstrated that nanomolar concentrations of auxin in the medium contacting the seedlings rescued the slow hypocotyl growth phenotype of *b19* seedlings (Figure 6b). Higher concentrations of IAA were inhibitory to both genotypes as previously documented (Collett *et al.*, 2000). A primary role of auxin in the control

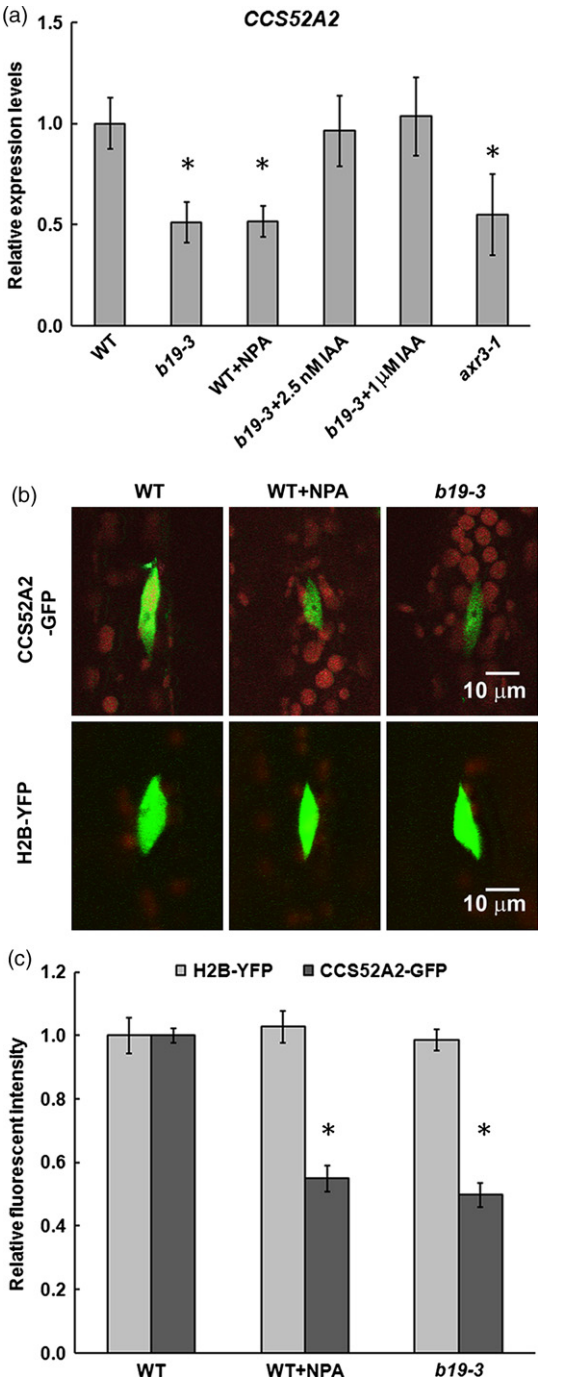

Figure 4. Lower *CCS52A2* expression in *b19* upper hypocotyls is due to defective auxin transport.
(a) qPCR analysis of *CCS52A2* expression in WT (Col-0) and *b19* seedlings. Error bars indicate standard error ($n = 3$ biological replicates). Significant differences between WT and mutants or WT with NPA treatment are indicated with * (P-value < 0.05).
(b) Confocal microscopy analysis of nuclear fluorescence intensity of CCS52A2–GFP and the histone-based nuclear marker H2B–YFP in the cortex of upper hypocotyls of Col-0 or *b19-3* treated with or without 1 μM NPA. Same chromophore has the same confocal setting. The backgrounds are chloroplasts.
(c) Quantification of fluorescence signal in nuclei like those shown in (b). Error bars indicate standard error of the mean ($n = 14–20$).

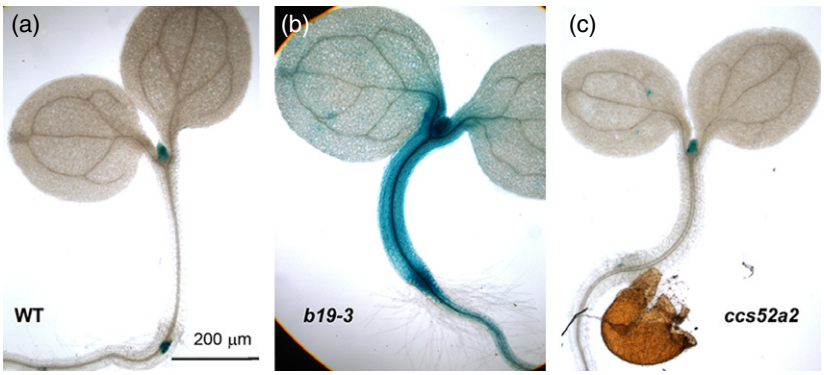

Figure 5. The expression of CYCB1;1-GUS is independent of CCS52A2.
GUS staining of CYCB1;1–GUS in the hypocotyl of WT (a), *b19-3* (b) and *ccs52a2* (c) mutant seedlings grown in 10 μmol m^{-2} sec^{-1} white light at 2.5 DAG.

of this phase of peak hypocotyl growth rate was further supported by showing that *axr2* and *axr3* auxin signaling mutants were impaired similar to or even more than *b19* mutants (Figure 6c), consistent with previously published hypocotyl end-point measurements (Nagpal *et al.*, 2000). If lower ploidy caused by reduced auxin flow to the growth zone reduces hypocotyl elongation then mutating *CCS52A2* while leaving *B19* intact would be expected to reduce hypocotyl growth rate. Figure 6(c) shows this to be the case. Furthermore, the low growth rate of a *ccs52a2* mutant could not be rescued by auxin, though high auxin (1 μM) had its normal inhibitory effect (Figure 6c). Apparently, low concentrations of auxin promote growth by a mechanism that involves CCS52A2 but the inhibitory effects of micromolar auxin occur independently of CCS52A2.

A *ccs52a2 b19-3* double mutant was created. Figure 6(c) shows its phenotype to be consistent with the sum of the two constituent components. Nanomolar levels of auxin promoted elongation to a small extent, presumably by rescuing the *b19* genetic component. It appears that auxin promotes hypocotyl growth through CCS52A2-dependent and CCS52A2-independent pathways.

Figure 7(a) co-plots cycle value and growth rate data both obtained 2.5–3 DAG with wild-type and *b19-3* seedlings with or without auxin, and data from an *axr3* mutant, all in the Col-0 genetic background. The data show a striking rescue of *b19* ploidy (cycle value) and growth rate by 2.5 nM auxin. Clearly, the nuclear endocycle and growth rate in the auxin-transport mutant are both auxin-limited. Supplying auxin at a level high enough to restore the deficiency but low enough to avoid inducing inhibition allowed this response to be quantified. The wild type is not auxin deficient and therefore did not respond with respect to either the cycle value or growth rate. The auxin-insensitive *axr3* mutant has a cycle value and growth rate pair similar to an auxin-deficient mutant (*b19*). A logarithmic relationship was obtained between ploidy (cycle value) and growth rate when the latter was measured over a period of development spanning from 2 to 5 days after germination and the former was altered by mutations, chemical treatments, or light (Figure 7b).

DISCUSSION

The extraordinarily high level and spatial spread of the CYCB1;1–GUS cell cycle marker in *b19* hypocotyls was the original observation that instigated this study. The widely used CYCB1;1–GUS reporter gene includes the D-box domain of the cyclin fused to the GUS coding sequence. It faithfully reports mitotic events in otherwise wild-type plants because the D-box is sufficient for recognition and degradation at the appropriate phase of the cell cycle by the APC/C ubiquitin ligase complex, which would be expected to contain one of the CCS52A substrate-recognition and activating proteins (Peters, 2002; Capron *et al.*, 2003; Marrocco *et al.*, 2009). For example, CYCA2;3 cyclin is inactivated by an APC/C that contains CCS52A1 (Boudolf *et al.*, 2009). The present work used a *ccs52a2* mutant to test the analogous hypothesis that CYCB1;1 is inactivated by an APC/C containing CCS52A2. The results did not support the hypothesis (Figure 5). Expression data did not identify an alternative CCS52 family member to play the role apparently ruled out for CCS52A2. Perhaps in the absence of CCS52A2, *CCS52A1* is induced to control CYCB1;1 and thereby provide an explanation for the results in Figure 5. Supporting this possibility is that an APC/C containing CCS52A1 was shown to degrade CYCB1;1 and promote the endocycle in Arabidopsis trichomes (Kasili *et al.*, 2010). Alternatively, auxin may suppress CYCB1;1 in hypocotyls, thereby promoting the endocycle, by a pathway that does not involve cell-cycle switch proteins such as CCS52A2.

The present work does not provide a molecular-level explanation of the wide-spread CYCB1;1–GUS phenotype in *b19,* except that it is a consequence of auxin deficiency. What appears to be a similar ectopic spread of the same CYCB1;1-GUS reporter is induced by ultraviolet-B radiation in Arabidopsis hypocotyls, a treatment that also suppresses hypocotyl elongation (Biever *et al.*, 2014). However, the effect of ultraviolet-B radiation on CYCB1;1

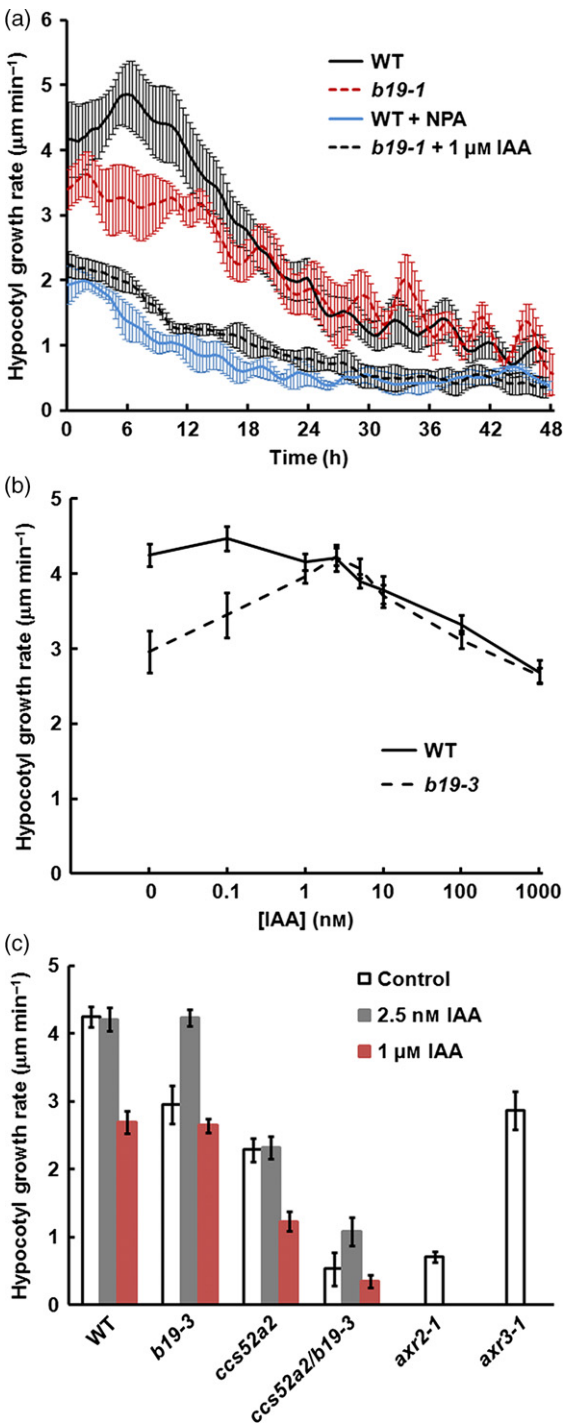

Figure 6. Auxin transport is required for hypocotyl elongation.
(a) High-resolution time courses of hypocotyl growth for 48 h beginning 2.5 days after germination under 10 μmol m^{-2} sec^{-1} white light. Images were automatically collected every 10 min and processed by a custom image analysis program. Error bars indicate standard error of the mean (n = 6–8 individuals for each genotype/treatment).
(b) Response of growth rate during the period of fastest elongation (2.5–3 days after germination) to dose of exogenous IAA in WT (Col-0) and *b19-3* seedlings (n > 20 per genotype/treatment).
(c) Nanomolar auxin restores low hypocotyl elongation of *b19*-3 but not *ccs52a2* mutants to WT (Col-0) levels (n > 20 per genotype/treatment).

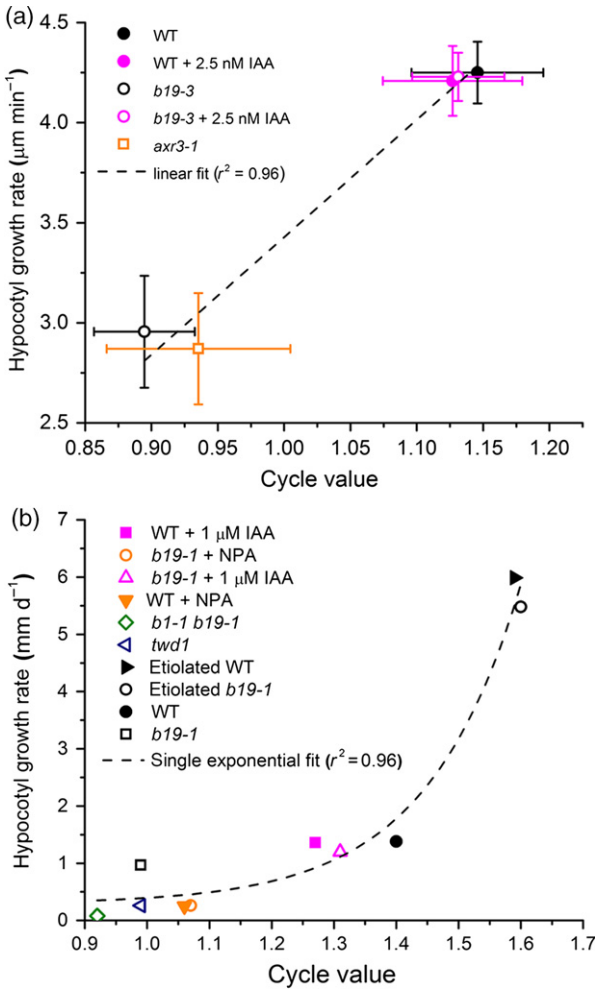

Figure 7. Positive relationships between cycle value and hypocotyl elongation rate.
(a) Hypocotyl elongation rate determined by computational analysis of images acquired over 12 h beginning with 2.5 DAG seedlings, and cycle value of nuclei extracted from the upper region of the hypocotyl. Auxin completely rescued the low growth/low cycle value of the *b19* mutant. The genotypes used were in the Col-0 background.
(b) Average growth rate obtained by measuring hypocotyl length from digital images acquired at 2.5 days and 5 days after germination, plotted as a function of cycle value in the indicated genotypes and treatments. The genotypes used were in the Ws background.

expression is explained by an increase in transcription (Biever *et al.*, 2014) whereas the auxin-deficiency effect on CYCB1;1 reported here cannot be explained by increased CYCB1;1 mRNA (Figure S1) and is probably a result of decreased protein degradation. Thus, the effects of ultraviolet-B radiation and impaired auxin transport on CYCB1;1 in hypocotyls are probably not mechanistically related.

The results presented here demonstrate that B19-mediated auxin transport affects CCS52A2 levels and endocycle activity in the upper hypocotyl (Figure 8), but the molecular mechanism is not yet clear. Transcript analysis of many cell-cycle regulators indicated that *CYCD4* genes

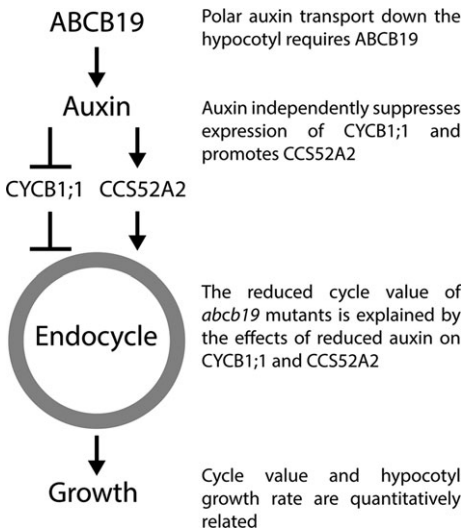

Figure 8. Structure of pathways connecting polar auxin transport to control of the endocycle and growth in the Arabidopsis hypocotyl that are consistent with the presented results.

should be considered in future studies of the mechanism. The lower transcript levels of *CYCD4;1* and *CYCD4;2* in *b19* mutants were restored to wild type by auxin treatment (Figure S1). Kono *et al.* (2007) showed that knockout and overexpression of *CYCD4* genes had major effects on cell division and differentiation in the epidermis of the Arabidopsis hypocotyl. Perhaps auxin regulation of *CYCD4* genes will be found to affect the endocycle and B19-dependent hypocotyl growth.

Regardless of the mechanism linking reduced CCS52A2 levels and reduced ploidy, there is a clear quantitative relationship between the endocycle and hypocotyl cell expansion (Figure 7). This is not the first evidence of a link between the endocycle and hypocotyl growth rate. Gendreau *et al.* (1998) used light quality and photomorphogenesis mutants to conclude that the photocontrol of hypocotyl elongation is exerted in part by controlling the endocycle. A defect in cell expansion in *bin4* mutant with a severe defect in endoreplication can be partially overcome by drug-induced tetraploidization (Breuer *et al.*, 2007). Other relevant research includes the finding that *CCS52A2* overexpression lines tend to have larger leaves with higher ploidy levels while mutation of *CCS52A2* causes dwarf plant and lower ploidy in leaves (Lammens *et al.*, 2008; Liu *et al.*, 2012).

Insufficient auxin availability due to impaired rootward transport is sufficient to explain the low levels of CCS52A2 in *b19* hypocotyls (Figure 8). Resupply of auxin at nanomolar or below concentrations rescues *b19* phenotypes, which may seem surprising given that auxin typically acts in the 0.1–1 μM range. However, the defect to be rescued in this case is the supply of the hormone to the deficient cells, which apparently use the nanomolar supply to create the appropriate internal concentrations using the proteins and thermodynamic gradients that govern auxin movement (Spalding, 2013). In fact, nanomolar treatments may be more effective at rescuing auxin deficiencies than micromolar concentrations because they may be less likely to trigger effects on transporter trafficking, internalization, and degradation (Friml, 2010).

In the present study, high auxin rescued the CYCB1;1 reporter phenotype and low ploidy of *b19* but not the hypocotyl growth phenotype. Instead, high auxin suppressed hypocotyl growth. Even the slow growth of *ccs52a2* hypocotyls was inhibited more by high auxin (Figure 6c). Therefore, promotion of growth by nanomolar concentrations of auxin requires CCS52A2 but the inhibitory action of high auxin does not.

Although the experiments reported here were performed in an organ mostly lacking cell division, the link between auxin transport, the endocycle, and cell expansion may be very relevant to the shoot and root apical meristems, as these are sites of high auxin and cell-cycle activity (Ishida *et al.*, 2010). In *Arabidopsis,* both *CCS52A1* and *CCS52A2* are reportedly required for root meristem maintenance (Vanstraelen *et al.*, 2009). *CCS52A1* controls meristem size by promoting endocycle and mitotic exit in the elongation zone. In contrast, *CCS52A2* is expressed at the distal part of the root meristem and required to maintain the stem cell identity in the quiescent center. *CCS52A2* is also required for shoot apical meristem maintenance by controlling mitotic activity (Liu *et al.*, 2012).

Decades of auxin studies led to the acid-growth hypothesis in which wall acidification due to H^+-ATPase activation promotes cell expansion at least in part by putting the wall-loosening expansin proteins in a permissive environment. Auxin activation of the H^+-ATPase in *Arabidopsis* involves phosphorylation (Takahashi *et al.*, 2012) over a time frame best measured in minutes. The experiments reported here have a different context. Rather than a mechanism that responds to a change in auxin distribution such as following tropic stimuli, the mechanism explored here relates more to a longer term steady state in which auxin flow down the hypocotyl coordinates cell-cycle activity to adjust ploidy as an element of growth control. A comprehensive understanding of hypocotyl elongation during seedling development will require integration of short term and steady state growth control mechanisms.

EXPERIMENTAL PROCEDURES

Plant material

The following *Arabidopsis thaliana* genotypes were used: wild-type plants of ecotypes Ws and Col-0; mutant *b19-1, b1b19* (Noh *et al.*, 2001); *b19-3* (Lewis *et al.*, 2007); *twd1-1* (Wu *et al.*, 2010b); *axr2-1* and *axr3-1* (Leyser *et al.*, 1996); *ccs52a2* (Vanstraelen *et al.*,

2009). Construction of *proCYCB1:1:CYCB1;1–GUS,* which contains the promoter and the destruction box (D-box) of *CYCB1;1* fused to the *uidA* gene, was described by Colón-Carmona *et al.* (1999). *CCS52A1–GFP* and *CCS52A2–GFP* constructs driven by native promoters, are previously characterized (Vanstraelen *et al.*, 2009). *H2B–YFP* was described by Boisnard-Lorig *et al.* (2001). All seedlings were grown on half-strength Murashige and Skoog medium under continuous 10 μmol m^{-2} sec^{-1} white light at 25°C. In the case of IAA or NPA treatment, the chemicals were included in the agar medium to which seeds displaying an emerged radicle were transferred, typically 1 day after a 2-day stratification period.

Confocal microscopy

Confocal microscopy was performed on a Zeiss LSM 510 laser scanning confocal microscope (Oberkochen, Germany) as described previously (Wu *et al.*, 2007). Fluorescence intensities and nuclear areas were measured from the acquired image files using Zeiss AIM software. Identical microscope and detector settings were used whenever fluorescence measurements were compared (Figures 2 and 4).

Flow cytometric analysis

Nuclei suspensions were prepared from average of 20–25 upper hypocotyls per sample, collected from 2.5 to 3 DAG seedlings using a surgical razor. Then tissues were chopped for 2–3 min in a drop of CyStain UV Ploidy solution (Partec GmbH, Germany) containing DAPI. Next, 2 ml more solution was added to the samples and the suspensions passed through 30 μm CellTrics filter (Partec). The ploidy was measured with BD LSR II flow cytometer using Lightwave Xcyte laser with 20 mW at 355 nm (BD Biosciences, San Jose, California, USA). In each run, average 5000 events were counted at a speed of 500 events min^{-1}. DAPI fluorescence histogram (Figure S1) was used to calculate ploidy levels using FlowJo software. The cycle value was calculated as described (Barow and Meister, 2003).

Hypocotyl length measurements and time course of hypocotyl growth

Growth rates presented in Figures 6 and 7 were measured from time-lapse digital images but by different methodologies depending on the goal. The extended time course of growth rate presented in Figure 6(a) was generated by tracking the growth of seedlings beginning 2.5 days after germination every 10 min for 48 h with the measurements extracted from the time series of images by the HYPOTrace computer program (Wang *et al.*, 2009). These results showed the peak growth rate of wild-type seedlings occurred approximately 4 h after the 2.5 DAG point. Therefore, the experiments shown in Figures 6(b, c) and 7(a) focused on this time period. Two images taken 3 h apart during this window were manually measured by ImageJ to determine how much each hypocotyl had changed in length during the interval. The growth rate data in Figure 7(b) were obtained by manually measuring the difference in hypocotyl lengths in images taken at 2.5 days and 5 days after germination.

Real-time RT-PCR analysis

Total RNA was extracted from the upper hypocotyl of 2.5–3 DAG seedlings using QIAGEN RNeasy Plant Total RNA Kit (Valencia, CA, USA). The RNA samples were first treated with DNase I and first strand cDNA was synthesized using Promega GoScript Reverse Transcription System. Quantitative PCR was performed using Promega Go*Taq* qPCR Master Mix (Madison, WI, USA) and Stratagene Mx3000p (Cedar Creek, TX, USA). *UBQ10* transcripts were also quantified to normalize the amount of total transcripts in each sample. The primers used in the study are listed in Table S1.

ACCESSION NUMBERS

The Arabidopsis Genome Initiative locus identifier for the *ABCB19* gene is *At3g28860, ABCB4* is *At2g47000, ABCB1* gene is *At2g36910,* and *TWD1* is *At3g21640.*

ACKNOWLEDGEMENTS

We thank Dagna Sheerar for assisting with flow cytometry, Matthew Mixdorf for assisting with the hypocotyl growth measurements, and Elizabeth Henry for help with the initial CYCB1;1 reporter measurements. We thank Eva Kondorosi and the ABRC for providing plant materials. This work was supported by National Science Foundation Grant IOS-0921071 to E.P.S.

AUTHOR CONTRIBUTIONS

G.W. and E.P.S. designed the experiments. G.W. performed all experiments with the assistance of J.C. G.W. and E.P.S analyzed the data. G.W. and E.P.S. wrote the article.

SUPPORTING INFORMATION

Additional Supporting Information may be found in the online version of this article.

Figure S1. Expression of various cyclin genes in WT and *b19* upper hypocotyls measured by qPCR.

Table S1. Primers for qPCR (Forward/Reverse).

REFERENCES

Bargmann, B.O.R. and Estelle, M. (2014) Auxin perception: in the IAA of the beholder. *Physiol. Plant.* **151**, 52–61.

Barow, M. and Meister, A. (2003) Endopolyploidy in seed plants is differently correlated to systematics, organ, life strategy and genome size. *Plant, Cell Environ.* **26**, 571–584.

Biever, J.J., Brinkman, D. and Gardner, G. (2014) UV-B inhibition of hypocotyl growth in etiolated *Arabidopsis thaliana* seedlings is a consequence of cell cycle arrest initiated by photodimer accumulation. *J. Exp. Bot.* **65**, 2949–2961.

Boisnard-Lorig, C., Colon Carmona, A., Bauch, M., Hodge, S., Doerner, P., Bancharel, E., Dumas, C., Haseloff, J. and Berger, F. (2001) Dynamic analyses of the expression of the HISTONE:YFP fusion protein in Arabidopsis show that syncytial endosperm is divided in mitotic domains. *Plant Cell*, **13**, 495–509.

Bouchard, R., Bailly, A., Blakeslee, J.J. *et al.* (2006) Immunophilin-like TWISTED DWARF1 modulates auxin efflux activities of *Arabidopsis* P-glycoproteins. *J. Biol. Chem.* **281**, 30603–30612.

Boudolf, V., Lammens, T., Boruc, J. *et al.* (2009) CDKB1;1 forms a functional complex with CYCA2;3 to suppress endocycle onset. *Plant Physiol.* **150**, 1482–1493.

Breuer, C., Stacey, N.J., West, C.E., Zhao, Y., Chory, J. Tsukaya, H., Azumi, Y., Maxwell, A., Roberts, K. and Sugimoto-Shirasu, K. (2007) BIN4, a novel component of the plant DNA topoisomerase VI complex, is required for endoreduplication in *Arabidopsis*. *Plant Cell*, **19**, 3655–3668.

Capron, A., Ökrész, L. and Genschik, P. (2003) First glance at the plant APC/C, a highly conserved ubiquitin-protein ligase. *Trends Plant Sci.* **8**, 83–89.

Cebolla, A., Vinardell, J.M., Kiss, E., Oláh, B., Roudier, F., Kondorosi, A. and Kondorosi, E. (1999) The mitotic inhibitor *ccs52* is required for endoreduplication and ploidy-dependent cell enlargement in plants. *EMBO J.* **18**, 101–109.

Chae, K., Isaacs, C.G., Reeves, P.H., Maloney, G.S., Muday, G.K., Nagpal, P. and Reed, J.W. (2012) *Arabidopsis SMALL AUXIN UP RNA63* promotes hypocotyl and stamen filament elongation. *Plant J.* **71**, 684–697.

Cleland, R.E. (1995) Auxin and cell elongation. In *Plant Hormones: Physiology, Biochemistry and Molecular Biology* (Davies, P.J., ed). Dordrecht, The Netherlands: Kluwer Academic Publishers, pp. 214–227.

Collett, C.E., Harberd, N.P. and Leyser, O. (2000) Hormonal interactions in the control of Arabidopsis hypocotyl elongation. *Plant Physiol.* **124**, 553–562.

Colón-Carmona, A., You, R., Haimovitch-Gal, T. and Doerner, P. (1999) Spatiotemporal analysis of mitotic activity with a labile cyclin-GUS fusion protein. *Plant J.* **20**, 503–508.

De Veylder, L., Beeckman, T. and Inzé, D. (2007) The ins and outs of the plant cell cycle. *Nat. Rev. Mol. Cell Biol.* **8**, 655–665.

De Veylder, L., Larkin, J.C. and Schnittger, A. (2011) Molecular control and function of endoreplication in development and physiology. *Trends Plant Sci.* **16**, 624–634.

Desvoyes, B., Fernandez-Marcos, M., Sequeira-Mendes, J., Otero, S., Vergara, Z. and Gutierrez, C. (2014) Looking at plant cell cycle from the chromatin window. *Front. Plant Sci.* **5**, 369.

Friml, J. (2010) Subcellular trafficking of PIN auxin efflux carriers in auxin transport. *Eur. J. Cell Biol.* **89**, 231–235.

Fülöp, K., Tarayre, S., Kelemen, Z., Horváth, G., Kevei, Z., Nikovics, K., Bakó, L., Brown, S., Kondorosi, A. and Kondorosi, E. (2005) Arabidopsis anaphase-promoting complexes: multiple activators and wide range of substrates might keep APC/C perpetually busy. *Cell Cycle*, **4**, 1084–1092.

Galbraith, D.W., Harkins, K.R. and Knapp, S. (1991) Systemic endopolyploidy in *Arabidopsis thaliana*. *Plant Physiol.* **96**, 985–989.

Geisler, M., Blakeslee, J.J., Bouchard, R. *et al.* (2005) Cellular efflux of auxin catalyzed by the Arabidopsis MDR/PGP transporter AtPGP1. *Plant J.* **44**, 179–194.

Gendreau, E., Traas, J., Desnos, T., Grandjean, O., Caboche, M. and Höfte, H. (1997) Cellular basis of hypocotyls growth in *Arabidopsis thaliana*. *Plant Physiol.* **114**, 295–305.

Gendreau, E., Höfte, H., Grandjean, O., Brown, S. and Traas, J. (1998) Phytochrome controls the number of endoreduplication cycles in the *Arabidopsis thaliana* hypocotyl. *Plant J.* **13**, 221–230.

Gutierrez, C. (2009) The Arabidopsis cell division cycle. *The Arabidopsis Book*, **7**, e0120. doi: 10.1199/tab.0120.

Ishida, T., Adachi, S., Yoshimura, M., Shimizu, K., Umeda, M. and Sugimoto, K. (2010) Auxin modulates the transition from the mitotic cycle to the endocycle in *Arabidopsis*. *Development*, **137**, 63–71.

Jensen, P.J., Hangarter, R.P. and Estelle, M.A. (1997) Auxin transport is required for hypocotyl elongation in light-grown but not in dark-grown Arabidopsis. *Plant Physiol.* **116**, 455–462.

Jovtchev, G., Schubert, V., Meister, A., Barow, M. and Schubert, I. (2006) Nuclear DNA content and nuclear and cell volume are positively correlated in angiosperms. *Cytogenet. Genome Res.* **114**, 77–82.

Kasili, R., Walker, J.D., Simmons, L.A., Zhou, J., De Veylder, L. and Larkin, J.C. (2010) SIAMESE cooperates with the CDH1-like protein CCS52A1 to establish endoreplication in *Arabidopsis thaliana* trichomes. *Genetics*, **185**, 257–268.

Kondorosi, E., Roudier, F. and Gendreau, E. (2000) Plant cell-size control: growing by ploidy? *Curr. Opin. Plant Biol.* **3**, 488–492.

Kono, A., Umeda-Hara, C., Adachi, S., Nagata, N., Konomi, M., Nakagawa, T., Uchimiya, H. and Umeda, M. (2007) The *Arabidopsis* D-type cyclin CYCD4 controls cell division in the stomatal lineage of the hypocotyl epidermis. *Plant Cell*, **19**, 1265–1277.

Lammens, T., Boudolf, V., Kheibarshekan, L., Panagiotis Zalmas, L., Gaamouche, T., Maes, S., Vanstraelen, M., Kondorosi, E., La Thangue, N.B. and Govaerts, W. (2008) Atypical E2F activity restrains APC/C/CCCS52A2 function obligatory for endocycle onset. *Proc. Natl Acad. Sci. USA*, **105**, 14721–14726.

Lewis, D.R., Miller, N.D., Splitt, B.L., Wu, G. and Spalding, E.P. (2007) Separating the roles of acropetal and basipetal auxin transport on gravitropism with mutations in two *Arabidopsis multidrug resistance-like* ABC transporter genes. *Plant Cell*, **19**, 1838–1850.

Leyser, H.M.O., Pickett, F.B., Dharmasiri, S. and Estelle, M. (1996) Mutations in the AXR3 gene of Arabidopsis result in altered auxin response including ectopic expression from the SAUR-AC1 promoter. *Plant J.* **10**, 403–413.

Liu, Y., Ye, W., Li, B., Zhou, X., Cui, Y., Running, M.P. and Liu, K. (2012) CCS52A2/FZR1, a cell cycle regulator, is an essential factor for shoot apical meristem maintenance in *Arabidopsis thaliana*. *BMC Plant Biol.* **12**, 135–149.

Marrocco, K., Thomann, A., Parmentier, Y., Genschik, P. and Criqui, M.C. (2009) The APC/C/C E3 ligase remains active in most post-mitotic Arabidopsis cells and is required for proper vasculature development and organization. *Development*, **136**, 1475–1485.

Melaragno, J.E., Mehrotra, B. and Coleman, A.W. (1993) Relationship between endopolyploidy and cell size in epidermal tissue of *Arabidopsis*. *Plant Cell*, **5**, 1661–1668.

Nagpal, P., Walker, L.M., Young, J.C., Sonawala, A., Timpte, C., Estelle, M. and Reed, J.W. (2000) AXR2 encodes a member of the Aux/IAA protein family. *Plant Physiol.* **123**, 563–574.

Noh, B., Murphy, A.S. and Spalding, E.P. (2001) *Multidrug resistance*-like genes of Arabidopsis required for auxin transport and auxin-mediated development. *Plant Cell*, **13**, 2441–2454.

Peters, J.-M. (2002) The anaphase-promoting complex: proteolysis in mitosis and beyond. *Mol. Cell*, **9**, 931–943.

Rayle, D.L. and Cleland, R.E. (1992) The Acid Growth Theory of auxin-induced cell elongation is alive and well. *Plant Physiol.* **99**, 1271–1274.

Santner, A. and Estelle, M. (2009) Recent advances and emerging trends in plant hormone signalling. *Nature*, **459**, 1071–1078.

Shaul, O., Nironov, V., Burssens, S., Montague, M.V. and Inze, D. (1996) Two *Arabidopsis* cyclin promoters mediate distinct transcriptional oscillation in synchronized tobacco BY-2 cells. *Proc. Natl Acad. Sci. USA*, **93**, 4868–4872.

Spalding, E.P. (2013) Diverting the downhill flow of auxin to steer growth during tropisms. *Am. J. Bot.* **100**, 203–214.

Spartz, A.K., Lee, S.H., Wenger, J.P., Gonzalez, N., Itoh, H., Inze, D., Peer, W.A., Murphy, A.S., Overvoorde, P. and Gray, W.M. (2012) The SAUR19 subfamily of *SMALL AUXIN UP RNA* genes promote cell expansion. *Plant J.* **70**, 978–990.

Sugimoto-Shirasu, K. and Roberts, K. (2003) "Big it up": endoreduplication and cell-size control in plants. *Curr. Opin. Plant Biol.* **6**, 544–553.

Takahashi, K., Hayashi, K. and Kinoshita, T. (2012) Auxin activates the plasma membrane H^+-ATPase by phosphorylation during hypocotyl elongation in Arabidopsis. *Plant Physiol.* **159**, 632–641.

Vanneste, S. and Friml, J. (2009) Auxin, a trigger for change in plant development. *Cell*, **136**, 1005–1016.

Vanstraelen, M., Baloban, M., Da Ines, O., Cultrone, A., Lammens, T., Boudolf, V., Brown, S.C., De Veylder, L., Mergaert, P. and Kondorosi, E. (2009) APC/C/C^{CCS52A} complexes control meristem maintenance in the *Arabidopsis* root. *Proc. Natl Acad. Sci. USA*, **106**, 11806–11811.

Wang, L., Uilecan, I.V., Assadi, A.H., Kozmik, C.A. and Spalding, E.P. (2009) HYPOTrace: image analysis software for measuring hypocotyl growth and shape demonstrated on *Arabidopsis* seedlings undergoing photomorphogenesis. *Plant Physiol.* **149**, 1632–1637.

Wu, G., Lewis, D.R. and Spalding, E.P. (2007) Mutations in *Arabidopsis Multidrug Resistance-Like* ABC transporters separate the roles of acropetal and basipetal auxin transport in lateral root development. *Plant Cell*, **19**, 1826–1837.

Wu, G., Cameron, J.N., Ljung, K. and Spalding, E.P. (2010a) A role for ABCB19-mediated polar auxin transport in seedling photomorphogenesis mediated by cryptochrome 1 and phytochrome B. *Plant J.* **62**, 179–191.

Wu, G., Otegui, M.S. and Spalding, E.P. (2010b) The ER-localized TWD1 immunophilin is necessary for localization of multidrug resistance-like proteins required for polar auxin transport in *Arabidopsis* roots. *Plant Cell*, **22**, 3295–3304.

Yang, T., Law, D.M. and Davies, P.J. (1993) Magnitude and kinetics of stem elongation induced by exogenous indole-3-acetic acid in intact light-grown pea seedlings. *Plant Physiol.* **102**, 717–724.

Zheng, B., Chen, X. and McCormick, S. (2011) The anaphase-promoting complex is a dual integrator that regulates both microRNA-mediated transcriptional regulation of cyclin B1 and degradation of cyclin B1 during Arabidopsis male gametophyte development. *Plant Cell*, **23**, 1033–1046.